IEEE Access
Multidisciplinary : Rapid Review : Open Access Journal

Received August 25, 2021, accepted September 25, 2021, date of publication September 29, 2021, date of current version October 6, 2021.

Digital Object Identifier 10.1109/ACCESS.2021.3116200

Influence of Inhomogeneous Residual Charges on the Stress of Filter Capacitor Components

PENGNING ZHANG[1], BOFAN LI[1], WEI LI[1], AND LIN LI[2], (Member, IEEE)
[1]School of Mechanical Electronic and Information Engineering, China University of Mining and Technology (Beijing), Beijing 100083, China
[2]State Key Laboratory of Alternate Electrical Power System with Renewable Energy Sources, North China Electric Power University, Beijing 102206, China

Corresponding author: Pengning Zhang (zpn2014@163.com)

This work was supported in part by the National Natural Science Foundation of China under Grant 52007192, and in part by the Fundamental Research Funds for the Central Universities under Grant 2020XJJD02.

ABSTRACT In recent years, the serious vibration and noise problem of high voltage filter capacitor has become the primary problem of noise reduction in high voltage direct current (HVDC) converter station. The current research mainly focuses on the experimental measurement of the vibration and noise of the filter capacitor, without considering the influence of the residual charge on the dielectric interface stress. In this paper, the experimental platform is built for measuring the residual charge of the dielectric film in filter capacitor component, and the measurement results show that there are non-uniform residual charges on the dielectric surface of filter capacitor. In order to study the influence of uneven distribution of charge on dielectric interface stress, 12 different residual charge distributions are designed, and the results show that the uneven distribution of surface residual charge has a great influence on dielectric interface stress, and the higher uneven distribution of residual charge can cause the larger the stress on the dielectric surface of filter capacitor. The negative residual charge can lead to larger dielectric interface stress, which has a more serious impact on the vibration of filter capacitor component.

INDEX TERMS Filter capacitor, unevenly distributed charge, vibration, stress.

I. INTRODUCTION

With the increasingly stringent environmental regulations, the noise pollution of filter capacitors in HVDC converter station has been widely concerned. CIGRE and IEC pointed out that the noise power level of filter capacitor can reach 105dB (A), which seriously exceeds the level of environmental protection [1]–[3]. Long term excessive vibration will also cause great damage to the capacitor structure, seriously reduce its service life and even resulting in huge economic losses. Therefore, the research on the internal vibration mechanism of filter capacitor can provide theoretical and data support for its vibration and noise reduction design, which has important engineering practical significance.

Cox and Guan calculates and analyzes the electric field force characteristics of the capacitor, and obtains that the electric field force of the capacitor is directly proportional to the square of the voltage [4]. A method for calculating the spectral noise of filter capacitors is proposed in [1] and [2]; The vibration of capacitor shell is related to the excitation frequency, and proposed to obtain the vibration of capacitor shell by calculating the frequency response function in [5] and [6]. A resonant vibration reduction measure based on a micro perforation plate (MPP) structure is first proposed [7]. Peng Wu has analyzed the noise reduction mechanism of the filter capacitor, and placed the compressible structure component (CSC) at the bottom of the capacitor to reduce the noise effectively [8]. Double bottom and foamed aluminum combination are also proposed in [9] and [10]. The vibration isolation measures are targeted to reduce the vibration propagation from the element package to the tank through increasing the elasticity of the propagation path.

The manufacturing process of filter capacitor component is shown in Fig. 1. Two layers of aluminum foil and six layers of polypropylene film are gathered together. After the spindle rotates and winds them to a certain length, they are flattened to form capacitor component. Therefore, in the manufacturing process of capacitor component, there will be residual charge on the dielectric film due to friction and winding. The current research shows that the plates inside the capacitor components are subject to the same force in the upper and lower directions, so that the forces on the plates

The associate editor coordinating the review of this manuscript and approving it for publication was Norbert Herencsar.

inside the capacitor cancel each other and are in a state of mechanical equilibrium. Only the outermost plate is subject to the downward force, and the innermost plate is subject to the upward force. Therefore, the electric field forces on the outermost and innermost plates cause the vibration of capacitor [4]–[6], [10]. However, the premise of the above conclusion is that there is no residual charge on the dielectric film of capacitor. Therefore, there is lack of research on the residual charge on the interface of dielectric film and the internal vibration mechanism of the capacitor component.

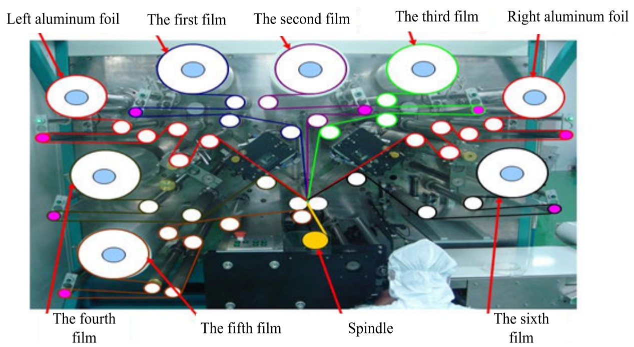

FIGURE 1. Manufacturing process of capacitor components.

The above researches on the vibration and noise of filter capacitor have made plentiful achievements, but the influence of the uneven residual charge on the internal force of filter capacitor is not studied. Therefore, it is necessary to further master the charge distribution law on the polyurethane film and analyze the influence of uneven residual charge on the stress of the capacitor component. In order to solve the above problems, the potential probe is used to measure the potential under each dielectric film of capacitor component, and the residual charge distribution on the surface of dielectric film is calculated by potential charge inversion method. Due to the uneven distribution of the residual charge on the dielectric surface, 12 cases are designed to study the influence of the residual charge with different uniformity and polarity on the dielectric force. The results will provide theoretical and data support for the research of the internal vibration mechanism of the filter capacitor.

II. MEASUREMENT OF RESIDUAL CHARGE

A. POTENTIAL MEASURING SET-UP

The potential under the polypropylene dielectric film of the capacitor is measured by EST-102 vibration capacitance electrometer in this paper. The electrometer is shown in Fig. 2. The range of the electrometer is 0- ± 200V, 0- ± 2kV, 0- ± 20kV, the highest resolution can reach 0.1V, and the measurement distance is 2 mm-100 mm. The distance between the potential probe and the dielectric film is 88 mm, and the diameter and length of the probe are 25 mm and 54 mm respectively. In order to ensure the accuracy of the experiment, the voltage coefficient of the electrometer has been calibrated according to the actual measurement distance before the experiment begins.

FIGURE 2. EST-102 vibrating capacitive electrometer.

In order to reduce the measurement error caused by operation, a probe motion control mechanism is designed and manufactured. The probe motion control mechanism is shown in Fig. 3. The mechanism includes X-axis and Y-axis tracks, and can accurately control the position of the probe through programming. The maximum measurement range of the probe is 800mm × 800mm. The polypropylene dielectric film is placed at a certain distance above the probe with a phenolic resin bracket, and the distance between the dielectric film and the probe is adjusted by changing the height of the phenolic resin bracket, so as to ensure the reliability of charge measurement. The experimental site of charge measurement of filter capacitor dielectric film is shown in Fig. 3.

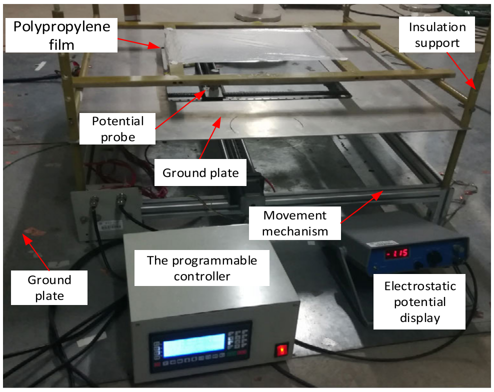

FIGURE 3. Set-up for measuring charge of dielectric film.

B. INVERSION CALCULATION OF SURFACE CHARGE OF DIELECTRIC FILM

Then the magnetostriction of the silicon steel, amorphous or nanocrystalline can be obtained by the measured acceleration.

After measuring the potential distribution at a certain distance below the dielectric film, the potential-charge inversion calculation method is generally adopted. The principle of this method is that the charge on the dielectric film will generate potential at any point P in the space, and the potential at point P in the space can be calculated by equation (1) [11].

$$\varphi(P) = \frac{1}{4\pi \varepsilon_0} \oint_S \frac{\sigma_a}{r} \mathrm{d}S \tag{1}$$

where r is the distance from a point on the surface of polypropylene dielectric film to point P in space, σ_a is the charge density. The total potential of any point P in space can be obtained by surface integral the potential of each point on the dielectric film to point P.

The surface of the dielectric film under test is divided into n elements. If n is large enough, the charge distribution on each element can be considered to be uniform. Therefore, the integral form of equation (1) can be simplified to the summation form.

$$\varphi(P) = \frac{1}{4\pi\varepsilon_0}\sum_{i=1}^{n}(\sigma_a)_i \oint_{S_f}\frac{1}{r}\,dS \tag{2}$$

where s_i is the area of the ith element on the dielectric film, so the potential of point P is the sum of the potentials generated by all the elements on the dielectric film.

The potential at a certain distance below the ith element can be calculated by equation (3).

$$\varphi_j = \frac{1}{4\pi\varepsilon_0}\sum_{i=1}^{n}(\sigma_a)_i \oint_{S_i}\frac{1}{r_{ij}}\,dS \tag{3}$$

where r_{ij} is the distance from the center point of the ith element on the dielectric film to the jth potential measuring point. Therefore, if the dielectric film is divided into n elements, n equations are listed and all equations are written in matrix form.

$$\begin{bmatrix} P_{11} & P_{12} & \cdots & P_{1n} \\ P_{21} & P_{22} & \cdots & P_{2n} \\ \vdots & \vdots & \ddots & \vdots \\ P_{n1} & P_{n2} & \cdots & P_{nn} \end{bmatrix} \begin{bmatrix} (\sigma_a)_1 \\ (\sigma_a)_2 \\ \vdots \\ (\sigma_a)_n \end{bmatrix} = \begin{bmatrix} \varphi_1 \\ \varphi_2 \\ \vdots \\ \varphi_n \end{bmatrix} \tag{4}$$

where the matrix on the left is the coefficient matrix P, that is the incidence matrix between the charge density on the surface of dielectric film and the potential below the element. The P_{ij} in the coefficient matrix P can be calculated by equation (5).

$$P_{ij} = \frac{1}{4\pi\varepsilon_0}\oint_{S_i}\frac{1}{r_{ij}}\,dS \tag{5}$$

If the coefficient matrix P is reversible, the charge can be obtained by inversion of the potential below the dielectric film.

$$\begin{bmatrix} (\sigma_a)_1 \\ (\sigma_a)_2 \\ \vdots \\ (\sigma_a)_n \end{bmatrix} = P^{-1}\begin{bmatrix} \varphi_1 \\ \varphi_2 \\ \vdots \\ \varphi_n \end{bmatrix} \tag{6}$$

According to the above principal analysis, the residual charge density on the surface of dielectric film can be calculated by MATLAB programming. When measuring the potential at a certain distance below the dielectric film, the dielectric film is evenly divided into n elements, and each element is a rectangular unit (as shown in Fig. 4). The n elements are numbered, and it is considered that a certain number of charges are evenly distributed on each element.

The capacitor component is made of six layers of dielectric film and two layers of aluminum foil. The structure of each layer of capacitor component is shown in Fig. 4 (a). The width of the component is 16cm. Three rolls of capacitor component are taken as the experimental object. The distribution of measuring points in the three rolls of dielectric film is shown in Fig. 4 (b), which is divided into 90 elements in total.

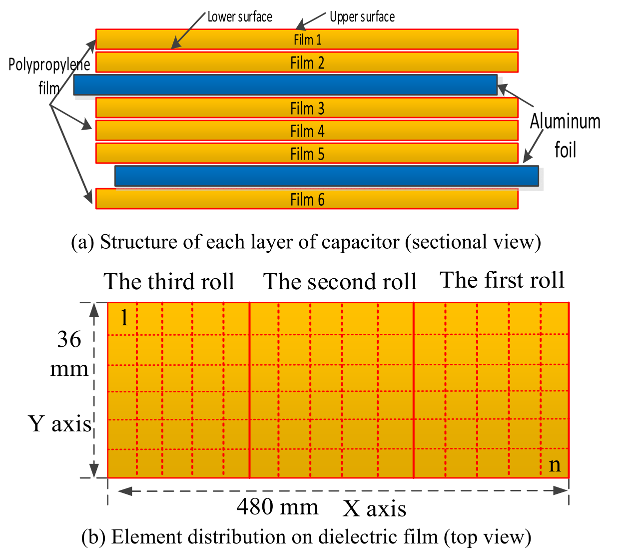

FIGURE 4. **The structure of each layer in the capacitor component and the distribution of measuring points.**

C. MEASUREMENT RESULTS OF RESIDUAL CHARGE

The total charge density of the first layer of polypropylene film is shown in Fig. 5 (a), and it can be seen that the maximum charge density on the polypropylene film is -2.34×10^{-5}C/m^2. The results show that the charge density on the two side parts is small and the charge density on middle part is large. In order to grasp the distribution of residual charge on the upper and lower surface of the dielectric film, the first film layer has been wiped with alcohol cotton. The charge on the upper surface dissipated during the process of wiping and alcohol volatilization. Therefore, the residual charge measured after wiping the upper surface of the dielectric film is the charge on the lower surface. The residual charge distribution on the lower surface of the first film is shown in Fig. 5 (b) after wiping alcohol. It can be seen that the maximum residual charge density of the lower surface of the first film is -1.69×10^{-6}C/m^2, compared with the total charge density of the first layer, it is reduced by about one order of magnitude.

The total charge of the second polypropylene film layer is shown in Fig. 5 (c). The charge of most of its area is negative, and the maximum charge density is -2.65×10^{-5}C/m^2. The charge distribution on the lower surface of the second polypropylene film layer is shown in Fig. 5 (d). It can be seen that the upper part of the lower surface is positive charge and the lower part is negative charge, and the maximum charge density is 1.05×10^{-6}C/m^2.

The total charge distribution of the third polypropylene film layer is shown in Fig. 5 (e). The charge of most of its area is positive, the charge density in the middle is greater than that around, and the maximum charge density is 2.55×10^{-5}C/m^2. The charge distribution on the lower surface of the third polypropylene film layer is shown in Fig. 5 (f), and the maximum charge density is 8.7×10^{-7}C/m^2.

The total charge distribution of the fourth polypropylene film layer is shown in Fig. 6 (a), the charge of most of its area is positive, and the maximum charge density is 2.3×10^{-5}C/m^2. The charge distribution on the lower surface of the fourth polypropylene film layer is shown in Fig. 6 (b), and the maximum charge density is 3.55×10^{-6}C/m^2.

The total charge distribution of the fifth polypropylene film layer is shown in Fig. 6 (c). The charge of most of its area is positive, and the maximum charge density is 1.14×10^{-5}C/m^2. The charge distribution on the lower surface of the fifth polypropylene film layer is shown in Fig. 6 (d), and the maximum charge density is -3.7×10^{-6} C/m^2.

The total charge distribution of the sixth polypropylene film layer is shown in Fig. 6 (e). The charge of most of its area is positive, but the maximum charge density is -2.47×10^{-5}C/m^2. The charge distribution on the lower surface of the sixth polypropylene film layer is shown in Fig. 6 (f), and the maximum charge density is -9.4×10^{-7} C/m^2. In conclusion, the measurement result shows that the polypropylene film of filter capacitor existences residual charge which cannot be ignored, and the maximum residual charge density is 2.65×10^{-5} C/m^2. At the same time, the charge distribution on the upper and lower surface of the film is especially different.

III. SIMULATION

The simulation model of a roll of capacitor components is shown in Fig. 7. The middle two layers of polyurethane film are divided into eight equal parts, each part is set to a different order of charge density. The two interfaces in the middle three-layer dielectric film are divided into 8 equal

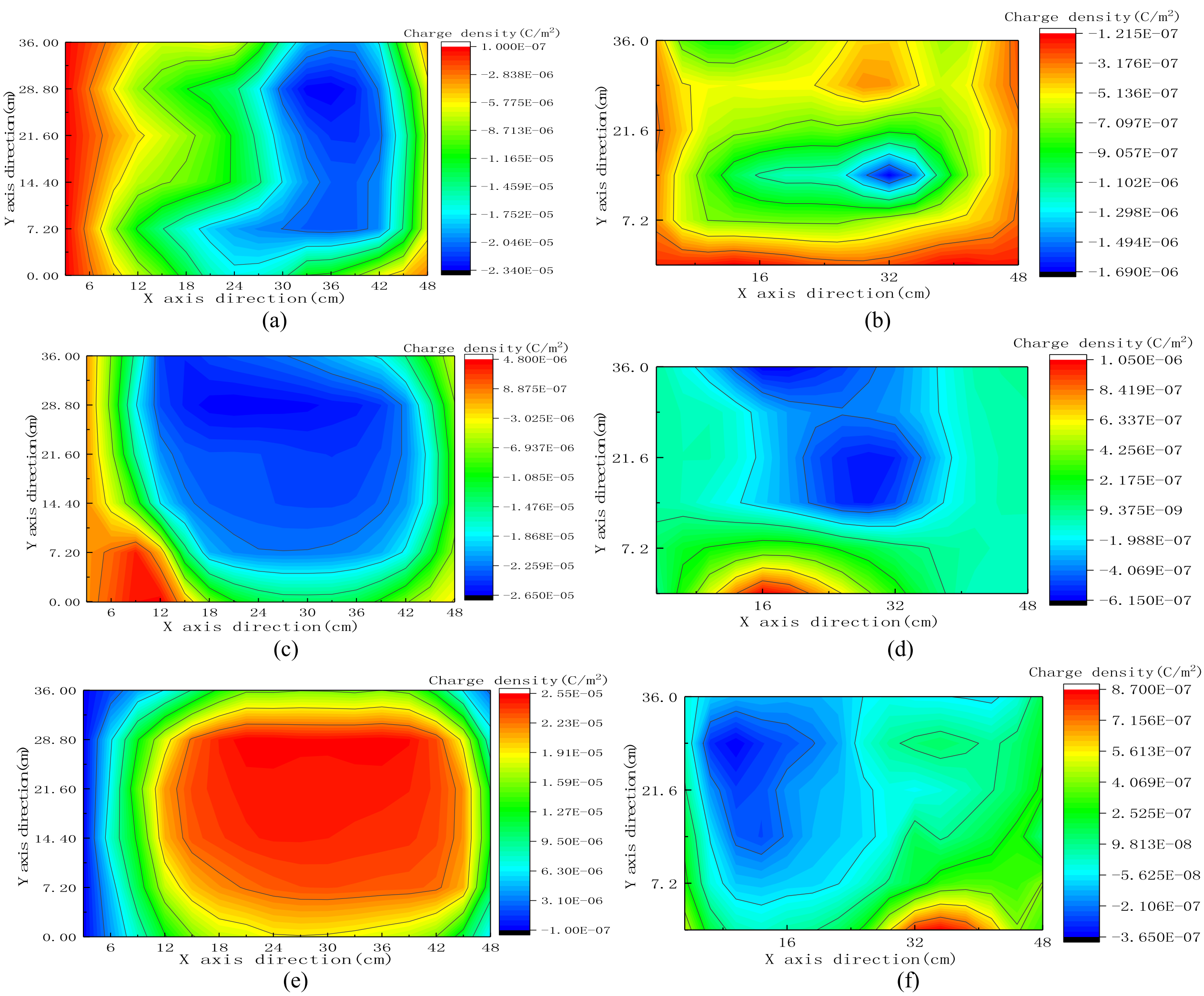

FIGURE 5. **Residual charge distribution on 1-3 layers of dielectric films.**

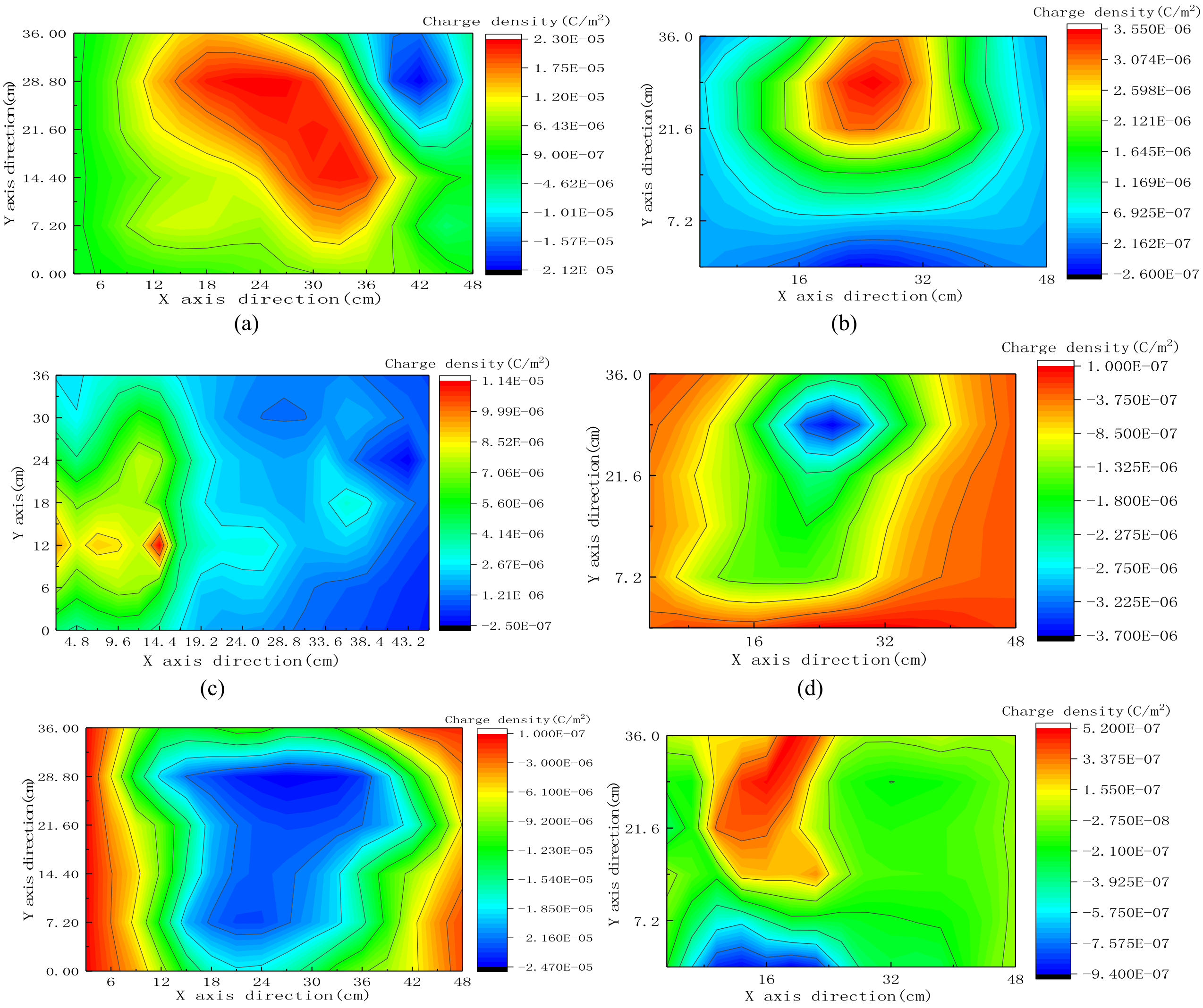

FIGURE 6. Residual charge distribution on 4-6 layers of dielectric thin films.

TABLE 1. Distribution of residual charge at dielectric interface.

Region / Case	1 (10^{-6})	2 (10^{-6})	3 (10^{-6})	4 (10^{-6})	5 (10^{-6})	6 (10^{-6})	7 (10^{-6})	8 (10^{-6})	Average (10^{-6})	uneven coefficient
Case 1	0	0	0	0	0	0	0	0	0	/
Case 2	1	1	1	1	1	1	1	1	1	1
Case 3	10	10	10	10	10	10	10	10	10	1
Case 4	100	100	100	100	100	100	100	100	100	1
Case 5	1.05	0.19	0.27	3.95	1.14	0.11	1.02	0.27	1	3.95
Case 6	3.72	9.94	30.1	2.74	21.8	6.8	3.15	1.88	10	3.01
Case 7	70.7	56.3	24.4	25.2	24.2	70.8	23.3	71.7	45.8	1.57
Case 8	20.7	6.33	74.4	85.2	64.2	20.8	73.3	21.7	45.8	1.86
Case 9	10.7	86.3	14.4	65.2	0	90.8	3.31	95.9	45.8	2.09
Case 10	69.2	90.5	56.5	160	91.8	35.1	200	99.4	100	1.99
Case 11	-1.05	-0.19	-0.27	-3.95	-1.14	-0.11	-1.02	-0.27	-1	3.95
Case 12	-70.7	-56.3	-24.4	-25.2	-24.2	-70.8	-23.3	-71.7	-45.8	1.57

Note: the unit of charge density is C/m^2.

parts. Residual charges of different magnitude are distributed in different subarea on the dielectric interface. The stress in the capacitor is calculated and analyzed.

In the converter station, the excitation voltage of filter capacitor bank in normal operation includes 50 Hz, 550 Hz and 650 Hz components. According to the normal operating conditions, in the simulation, the capacitor excitation voltage is set as follows: the amplitude of 50 Hz voltage excitation is 2100 V, the amplitude of 550 Hz voltage excitation is 550 V, and the amplitude of 650 Hz voltage excitation is 30 V.

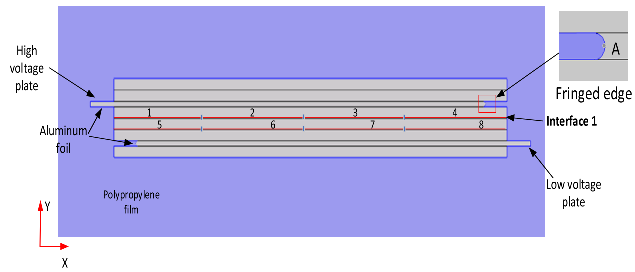

FIGURE 7. The simulation model.

Through the charge measurement experiment of capacitor dielectric film, it can be seen that there are extremely uneven residual charges on the dielectric film of filter capacitor. The relative dielectric constants of dielectric films are the same, and the residual charges density is σ between two layers of the dielectric films, the boundary condition on the interface between two film layers can be expressed as:

$$\boldsymbol{a}_n \cdot (\boldsymbol{D}_2 - \boldsymbol{D}_1) = \sigma \tag{7}$$

where $\boldsymbol{D}$ is the electric displace vector, and $\boldsymbol{a}_{\mathrm{n}}$ is the normal unit vector on the interface. The equation (7) can be simplified as follows.

$$D_{2n} - D_{1n} = \sigma \tag{8}$$

From the equation $\boldsymbol{D} = \varepsilon \boldsymbol{E}$, it can be concluded as follows.

$$E_{2n} - E_{1n} = \frac{\sigma}{\varepsilon} \tag{9}$$

where $D_{1\mathrm{n}}$ and $D_{2\mathrm{n}}$ are vertical electric displacement vectors in the polypropylene film on both sides of the interface, $E_{1\mathrm{n}}$ and $E_{2\mathrm{n}}$ are vertical electric field strength in the polypropylene film. According to formula (9), when the residual charge is contained on the interface, the electric field strength in the polypropylene film on both sides of the interface is not equal, so the upward and downward forces of the aluminum foil cannot be offset.

In order to study the influence of the inhomogeneity of the interface charge on the force of dielectric film and conductor, the inhomogeneity coefficient of the charge is defined as follows.

$$\eta_e = \frac{\sigma_{\max}}{\sigma_{av}} \tag{10}$$

where $\sigma_{\max}$ is the maximum charge and σ_{av} is the average charge on the dielectric film.

In order to study the influence of the uneven distribution of charge on the dielectric force inside the capacitor, 12 different charge distributions are assumed, and the specific distribution data are shown in Table 1. It can be seen from Tab. 1 that the residual charge of the interface of the dielectric film is evenly distributed in case1, case2, case3 and case4, and the charge values are 0 C/m^2, 10^{-6} C/m^2, 10^{-5} C/m^2 and 10^{-4} C/m^2 respectively. The charges of case 5, case 6 and case 10 are unevenly distributed at the interface. The average charges at the interface of case 5, case 6 and case 10 are 10^{-6}C/m^2, 10^{-5}C/m^2 and 10^{-4}C/m^2 respectively.

The stress on the dielectric film and conductor of the capacitor component under six cases are calculated, the stress in X-direction of point A at the folded edge of conductor is shown in Fig. 8. It can be seen that the stress of point A in case 2 and case 5 are 3.820×10^5 Pa and 3.832×10^5 Pa respectively at 15.9 ms. In case 3 and case 6, the stress of point A is 3.839×10^5 Pa and 3.834×10^5 Pa respectively. In case 4 and case 10, the stress of point A is 4.05×10^5 Pa and 4.15×10^5 Pa respectively. It can be seen from the above results that the uneven distribution of residual charges on the dielectric surface has a certain influence on the stress of folded edge of conductor. The larger the average charge density on the dielectric surface have greater influence on stress of folded edge of conductor.

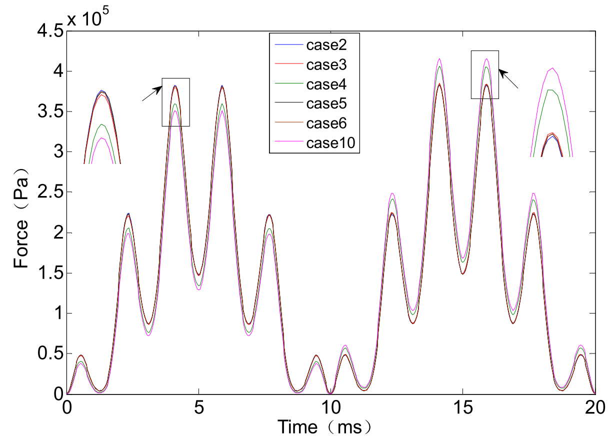

FIGURE 8. The stress in X-direction of point A at the folded edge of conductor.

At 4.1ms, the stress in Y direction of interface 1 under six cases is shown in Fig. 9. It can be seen that the stress at 0.43m of dielectric interface in case 2 and case 5 is 5.5×10^4 Pa and 5.56×10^4 Pa respectively. The results show that when the average charge is 10^{-6} C/m^2, the uneven distribution of charge has little effect on the stress of dielectric interface. In case 3 and case 6, the stress at 0.43m of dielectric interface is 5.5×10^4 Pa and 5.56×10^4 Pa respectively, the influence of the unevenly distributed charge on the surface force increases. In case 4 and case 10, the stress at 0.43m of dielectric interface is 4.9×10^4 Pa and 4.6×10^4 Pa respectively, the unevenly distributed charge has a great influence on the stress of the dielectric surface. Compared with case 3 and case 4, the stress

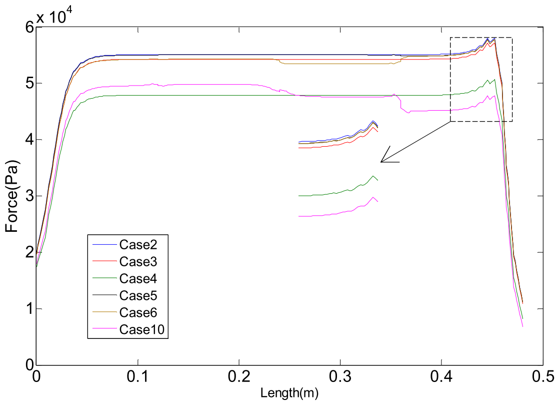

FIGURE 9. **The stress in Y direction of interface 1 at 4.1ms.**

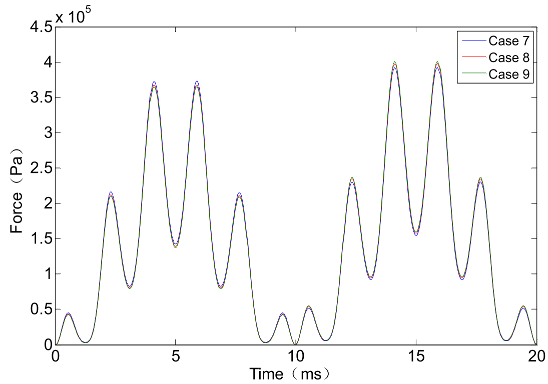

FIGURE 11. **The stress curve of point A.**

curves of case 6 and case 10 fluctuate greatly, which indicates that the uneven distribution of charges will lead to the uneven vibration of the dielectric surface.

At 4.1ms, the stress on the conductor surface under six conditions is shown in Fig. 10. It can be seen that the stress on both ends of the conductor fluctuates greatly, which is due to the existence of edge effect and the high electric field strength. The stress in the middle of the conductor is relatively stable, and the force in the middle of the conductor also fluctuates due to the influence of uneven distribution of charges.

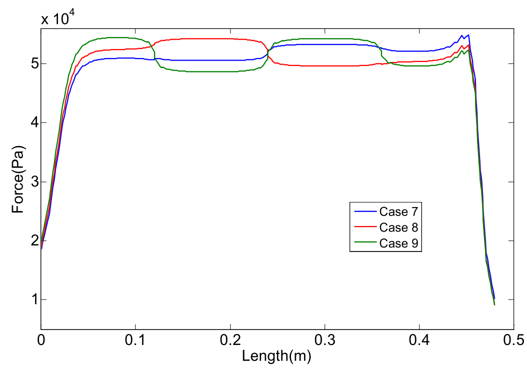

FIGURE 12. **The force in Y-direction of the interface 1 at 4.1ms.**

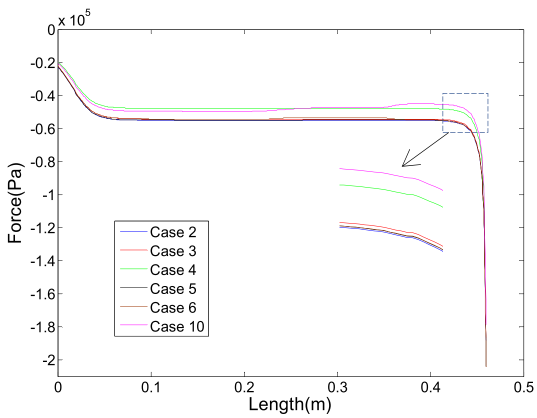

FIGURE 10. **The stress on the conductor surface at 4.1ms.**

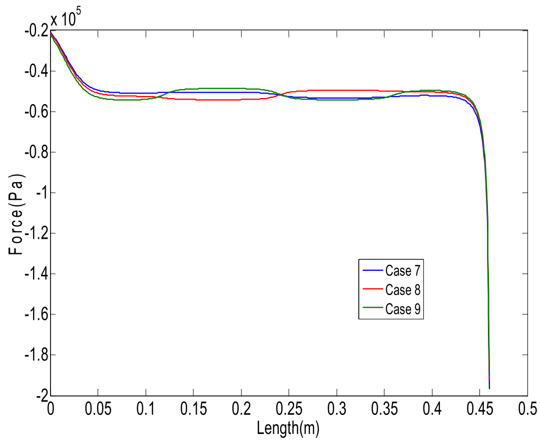

FIGURE 13. **The stress on the conductor at 4.1ms.**

The average charge density at the interface of case 7, case 8 and case 9 is 4.58×10^{-5} C/m^2, the charge inhomogeneity coefficient are 1.57, 1.86 and 2.09 respectively. Under three different cases, the stress curve of point A is shown in Fig. 11. It can be seen that the stress of point A in case 7, case 8 and case 9 is 3.925×10^5 Pa, 3.976×10^5 Pa and 4.1×10^5 Pa at 15.9 ms, which indicating that the greater charge inhomogeneity coefficient will cause the greater force on the dielectric interface.

In case 7, case8 and case9, the force in Y-direction of the interface 1 at 4.1ms is shown in Fig. 12. It can be seen that the stress fluctuation of interface 1 is the largest in case 9, the fluctuation of the stress at the interface is the smallest in case 7, which indicates that the more uneven residual charge at the interface can cause the greater stress fluctuation and have greater influence on the non-uniform vibration of the capacitor components.

In case 7, case8 and case9, the stress on the conductor at 4.1ms is shown in Fig. 13. It can be seen that the stress fluctuation of the conductor is still the largest in case 9, and the stress fluctuation of the conductor is the smallest in case 7, which indicates that the unevenly distributed residual charge

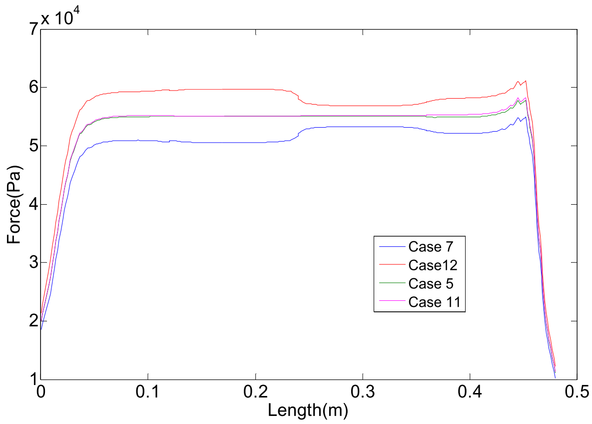

FIGURE 14. The stress on the interface 1 at 4.1ms.

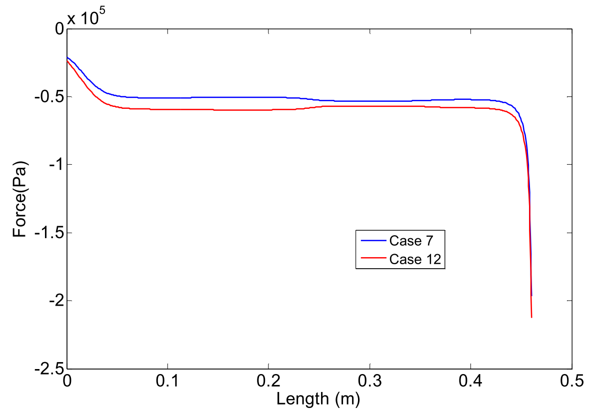

FIGURE 15. The stress on the conductor in case 7 and case 12 at 4.1ms.

at the dielectric interface also has a great influence on the stress of conductor.

In order to study the effect of negative residual charge on the force of capacitor component, case 11 and case 12 are added. The average charge density of case 11 and case 12 is -1×10^{-6}C/m^2 and -4.58×10^{-5} C/m^2 respectively. At 4.1ms, the stress on the interface 1 of case 7, case 12, case 5 and case 11 is shown in Fig. 14. It can be seen that the stress on the interface 1 of case 5 and case 11 is almost the same. But in case 12, the stress on the interface1 at 0.1m is 5.94×10^4 Pa. In case7, the stress at 0.1m is 5.083×10^4 Pa, which indicating that the residual charge of negative polarity has a greater influence on the force of capacitor components.

At 4.1ms, the stress on the conductor in case 7 and case 12 is shown in Fig. 15. It can be seen that the influence of negative residual charge on the stress of conductor is obviously greater than that of positive residual charge.

IV. CONCLUSION

In recent years, the noise problem of filter capacitor has become the primary problem of noise reduction in HVDC converter station. At present, the research mainly focuses on the experimental measurement of the vibration and noise of the filter capacitor, without considering the residual charge at the dielectric film interface. In this paper, the residual charge on the dielectric surface and the stress mechanism inside the filter capacitor component are studied, the main conclusions are summarized as follows:

(1) There is no obvious law of residual charge distribution on the dielectric interface of filter capacitor, and the charge distribution is extremely uneven. At the same time, the charge distribution on the upper and lower surface of the dielectric film is also extremely different.

(2) Compared with the uniformly distributed residual charge, the uneven distribution of residual charge on the dielectric surface has a greater impact on the stress of the capacitor component, which will lead to more severe vibration and greater noise of the capacitor.

(3) When the charge density is less than 10^{-6} C/m^2, the inhomogeneity of the charge distribution has little effect on the fluctuation of the stress of dielectric film. When the charge density is in the order of 10^{-5} C/m^{2}and 10^{-4} C/m^2, the larger inhomogeneous charge distribution will lead to the more serious inhomogeneous stress of dielectric film.

(4) Compared with the positive residual charge, the negative residual charge on the dielectric film will lead to greater stress on the capacitor component and more serious impact on the vibration of the capacitor.

REFERENCES

[1] *HVDC Stations Audible Noise*, CIGRE, Paris, France, 2002.
[2] *High Voltage Direct Current (HVDC) Substation Audible Noise*, Standard IEC-TS61973, 2012.
[3] A. Roget, "Study of vibration and audible noise generated by shunt capacitor banks at substations serving non-linear loads," M.S. thesis, Dept. Elect. Eng., Univ. Alabama, Tuscaloosa, AL, USA, 2011.
[4] M. D. Cox and H. H. Guan, "Vibration and audible noise of capacitors subjected to nonsinusoidal waveforms," *IEEE Trans. Power Del.*, vol. 9, no. 2, pp. 856–862, Apr. 1994.
[5] L. Zhu, S. Ji, Q. Shen, Y. Liu, J. Li, and H. Liu, "A noise level prediction method based on electro-mechanical frequency response function for capacitors," *PLoS ONE*, vol. 8, no. 12, Dec. 2013, Art. no. e81651.
[6] L. Zhu, J. Li, Y. Shi, H. Rehman, and S. Ji, "Audible noise characteristics of filter capacitors used in HVDC converter stations," *IEEE Trans. Power Del.*, vol. 32, no. 5, pp. 71–2263, Jul. 2017.
[7] W. Peng, J. Shengchang, C. Tao, L. Yanming, L. Xiaolin, and L. Yan, "Study on an audible noise reduction measure for the filter capacitors in the HVDC converter station based on the MPP absorber," *IEEE Trans. Power Del.*, vol. 24, no. 4, pp. 1756–1762, Oct. 2009.
[8] W. Peng, J. Shengchang, L. Yanming, and C. Tao, "Study on an audible noise reduction measure for filter capacitors based on compressible space absorber," *IEEE Trans. Power Del.*, vol. 26, no. 1, pp. 438–445, Jan. 2011.
[9] P. Wu, "Study on vibration and audible noise of AC-filter capacitors in HVDC converter station and control technology," Ph.D. dissertation, School Elect. Eng., Univ. Univ. Xi'an Jiaotong, Beilin, Xi'an, China, 2011.
[10] L. Zhu, "Study on noise prediction technology and reduction measures for AC filter capacitor installations in converter stations," Ph.D. dissertation, School Elect. Eng., Univ. Xi'an Jiaotong, Beilin, Xi'an, China, 2014.
[11] H. Ootera and K. Nakanishi, "Analytical method for evaluating surface charge distribution on a dielectric from capacitive probe measurement-application to a cone-type spacer in ±500 kV DC-GIS," *IEEE Trans. Power Del.*, vol. 3, no. 1, pp. 165–172, Jan. 1988.

PENGNING ZHANG was born in Yantai, China, in 1991. He received the Ph.D. degree in electrical engineering from North China Electric Power University, Beijing, in 2019. He has been a Lecturer with the School of Mechanical Electronic and Information Engineering, China University of Mining and Technology (Beijing), since 2019. His research interests include research on electromagnetic, vibration, and noise analysis on electromagnetic equipment.

BOFAN LI was born in Jiangsu, China, in 1995. He received the bachelor's degree in electrical engineering from China University of Mining and Technology (Beijing), where he is currently pursuing the master's degree. His research interest includes multi-physical field coupling calculation of high frequency transformer.

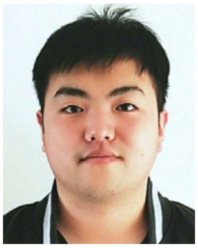

WEI LI was born in Tangshan, China, in 1996. He received the bachelor's degree in electrical engineering from Hebei University of Science and Technology. He is currently pursuing the master's degree with China University of Mining and Technology (Beijing). His research interest includes optimal design of high frequency transformer.

LIN LI (Member, IEEE) was born in China, in 1962. He received the Ph.D. degree in electrical engineering from North China Electric Power University, Baoding, Hebei, China, in 1997. He was a Visiting Scholar with the University of Florida, from 2006 to 2007. He has been a Professor with the School of Electrical and Electronic Engineering, North China Electric Power University, since 2001. His research interests include the fields of electromagnetic compatibility and electromagnetic-field theory and applications.